Systematic determination of bias and scatter in different experimental modal analysis methods

M. Böswald, M. Tang, R. Volkmar, K. Soal
DLR, German Aerospace Center, Institute of Aeroelasticity,
Bunsenstr. 10, 37073 Göttingen, Germany

Abstract
Experimental modal analysis is a tool to identify mathematical substitute models from measured vibrations for applications such as response prediction, controller design, and model validation. Since vibration measurements are affected by noise, the quality of the identified substitute models depends on the signal-to-noise ratio. Noise can cause stochastic errors (scatter) and systematic errors (bias) in the estimated modal parameters. This paper investigates the extent of scatter and bias with noisy input data for three representative modal analysis methods: the Least-Squares Complex Frequency-Domain (LSCF) estimator, the Least-Squares Complex Exponential (LSCE) estimator, and the Eigensystem Realization Algorithm (ERA). These methods represent different frequency- and time-domain identification approaches. Bias and scatter of the identified modal parameters (i.e. eigenfrequency, damping ratio, residue, modal mass) are evaluated systematically with noise for these methods in a Monte Carlo study using an analytical system.

1 Introduction

Vibrations play a crucial role in the design and certification of aeronautical structures. To mitigate development risks, validation of the finite element models of an aircraft is mandatory. To this end, ground vibration tests (GVTs) are performed on fully assembled prototypes. Afterwards, flight vibration tests are conducted to experimentally demonstrate freedom from flutter throughout the entire flight envelope.

A ground vibration test is carried out on a complex structure consisting of numerous interconnected components and characterized by high modal density. Typically, hundreds of response sensors are installed to capture the dynamic behavior of the structure. Artificial excitation is applied while the aircraft is on the ground, and multiple excitation configurations are used to ensure sufficient strength of excitation for all relevant modes within the frequency range of interest.

In practice, however, not all modes are equally well excited during every measurement run. Likewise, not all sensors exhibit a strong response in each test configuration. Furthermore, long cable distances and low electrical signal levels can result in a poor signal-to-noise ratio (SNR). Consequently, the measured data are affected by stochastic measurement errors that may influence the results of modal parameter estimation.

The central question addressed in this work is how sensitive modal analysis results are to such stochastic errors in the input data. This has been studied previously e.g. in [1] for operational modal analysis (OMA) with Stochastic Subspace Identification (SSI) for an application in civil engineering. The results and findings were obtained for one dedicated estimator on this specific application. They cannot be transferred easily to other parameter estimators or to other applications. In [2], an investigation on the confidence intervals of experimental modal analysis (EMA) has been conducted with the Least-Squares Complex Frequency-Domain (LSCF) estimator. A simple analytical system with two complex poles and residues was investigated in a Monte Carlo simulation. 500 realizations of frequency response functions (FRFs) contaminated with superimposed noise were analyzed for different SNR levels. The mean value and the variance are obtained for the identified modal parameters obtained with different implementations of

frequency-domain estimators. Again, results are obtained for frequency-domain estimators for a dedicated analytical system. It remains difficult to transfer the findings to other applications or other estimators.

In order quantify the uncertainties of different modal parameter estimators on the same test case and to be able to transfer findings to other applications, a systematic investigation is conducted here on a single-degree-of-freedom system with standardized analysis conditions. Both, time-domain and frequency-domain estimators are considered, while the level of noise contamination is varied. The errors are observed for all modal parameters identified. The error of the mean value and the coefficient of variation are determined for eigenfrequencies, damping ratios, residues and modal mass (i.e. extracted from the residue). In addition, the coefficient of correlation is determined between the identified eigenfrequencies and damping ratios.

The research procedure of this paper follows the investigations presented in chapter 5.8.1 of [3]. The use of standardized conditions shall however facilitate the transfer of the findings from the single-degree of freedom test case investigated here to well-separated modes of multi-degree-of-freedom systems. Ultimately, the results should enable modal analysis engineers to assess the accuracy of identified modal parameters based on an estimate of the signal-to-noise ratio of the measurement data.

In chapter 2 of this paper, the different modal parameter estimators are indicated with references for their theoretical foundations. The generation of stochastic datasets as baseline for the investigations is presented in chapter 3. The analysis of these stochastic datasets is carried out in chapter 4. Finally, chapter 5 summarizes the paper with some conclusions.

2 Different modal analysis methods

Different parameter estimators for experimental modal analysis are investigated in this paper with respect to the sensitivity of the results they provide due to stochastic measurement errors in the input data. Experimental modal analysis methods can be grouped into different categories: i) time- and frequency-domain methods, ii) single- and multi-degree of freedom methods, iii) modal and direct methods, etc. The methods investigated here are multi-degree of freedom methods from time-domain, i.e. the Least-Squares Complex Exponential (LSCE, see e.g. [4]) method and Eigensystem Realization Algorithm (ERA, see e.g. [5]), and from frequency-domain, i.e. Least-Squares Complex Frequency-Domain (LSCF, see e.g. [6]). Multi-degree of freedom means that the modal parameters of multiple modes are identified simultaneously and modal coupling is taken into account. Moreover, LSCE and LSCF are so-called modal methods, because the model equation for the parameter identification is derived from a modal equation of motion. On the other hand, ERA is a direct method and is based on a discrete-time state-space representation of a dynamic system. A discussion of the theoretical foundation of these methods is beyond the scope of this paper. Details of all three methods can be found e.g. in [3]. The theoretical backgrounds of LSCE and LSCF are well explained in [7]. A detailed discussion of the theory of ERA can be found in [8].

3 Generation of stochastic datasets

In this section, the generation of stochastic datasets for the investigation of the results sensitivity of the aforementioned modal parameter estimators is described. For the frequency-domain method LSCF, the synthesis of the FRFs for an analytical system and the subsequent contamination with noise in the frequency-domain is presented. For the time-domain methods LSCE and ERA, the generation of impulse response functions (IRFs) for an analytical system with the corresponding process of noise contamination in the time-domain is shown.

3.1 Normalized conditions and signal-to-noise ratio

One major objective of this research is to provide information about the errors in modal parameter estimation as a function of noise contamination of the input data. For assessment of errors in modal analysis results, an

analytical system has to be used whose modal parameters are known exactly. The normalization of modal analysis conditions is required in order to transfer the findings to general problems of modal identification. When using generic multi-degree of freedom systems, there are always multiple modes appearing in a frequency band with different strengths of excitation and thus different magnitudes of the corresponding resonance peaks in the FRFs. Consequently, the level of accuracy of the modal analysis results would differ for those modes, even if the same noise floor is added to analytical FRFs. To this end, it was decided to conduct the research on a single-degree of freedom system, where the signal-to-noise ratio can be controlled easily for a single modal response contribution. The properties of the analytical single-degree of freedom system used in the following are summarized in Table 1.

Table 1: Modal properties of analytical single-degree of freedom system

undamped eigenfrequency $f_r=\omega_r/(2\pi)$	10 Hz
viscous damping ratio D_r	0.02=2 %
modal mass m_r	1 kg m²
real-valued residue R_{kl}	1 kg^{-1}

In order to emulate stochastic measurement errors, noise is added to the response data of the analytical single-degree of freedom system. The strength of the noise contamination is controlled by the signal-to-noise ratio (SNR), with definition adopted from [9]. It is assumed that the measured time-domain IRF $h_{meas}(t)$ is a superposition of the noise-free IRF $h(t)$ and the zero-mean Gaussian white noise signal $n(t)$:

$$h_{meas}(t) = h(t) + n(t) \tag{1}$$

The SNR is determined from the ratio of the average power of these signals, which is calculated from the root-mean-square (RMS) of the sampled signals with $i=1, \ldots, N$ samples in the considered time interval:

$$SNR = \frac{\overline{P}_h}{\overline{P}_n} = \frac{h_{RMS}^2}{n_{RMS}^2} \tag{2}$$

$$h_{RMS} = \sqrt{\frac{1}{N}\sum_{i=1}^{N} h_i^2} \;,\; n_{RMS} = \sqrt{\frac{1}{N}\sum_{i=1}^{N} n_i^2} \tag{3}$$

A corresponding expression of SNR in the frequency-domain can be obtained when the time-domain signals are represented by superpositions of harmonic components, as it is exploited in discrete Fourier transform (DFT). The frequency-domain representation of the IRF is the FRF. Thus, the following relation is used to calculate the SNR of FRFs:

$$SNR = \frac{\overline{P}_H}{\overline{P}_N} = \frac{\sum_{i=1}^{n} \left| H(j\Omega_i) \right|^2}{\sum_{i=1}^{n} \left| N_i \right|^2} \tag{4}$$

In this equation, $N_i=N_{i,re} + jN_{i,im}$ represents the complex magnitude of the noise at the spectral line Ω_i. The real part and the imaginary part of the noise N_i over frequency Ω_i in the considered frequency band with $i = 1, 2, \ldots, n$ spectral lines are both uncorrelated Gaussian white noise with zero mean. When comparing signals with high dynamic range, it is common practice to express the SNR in decibels [dB]. Since signal power values are used here, the following equations apply in time-domain or in frequency-domain:

$$SNR_{dB} = 10dB \log\left(\frac{\overline{P}_h}{\overline{P}_n}\right) = 10dB \log\left(\frac{\sum_{i=1}^{N} h_i^2}{\sum_{i=1}^{N} n_i^2}\right) \tag{5}$$

$$SNR_{dB} = 10dB \log\left(\frac{\bar{P}_H}{\bar{P}_N}\right) = 10dB \log\left(\frac{\sum_{i=1}^{n}\left|H(j\Omega_i)\right|^2}{\sum_{i=1}^{n}\left|N_i\right|^2}\right) \tag{6}$$

This definition of SNR is used in the following to control the impact of Gaussian white noise on analytical response data. It should be mentioned that according to this SNR definition, the impact of noise is significant in case of low SNR values, like 10dB or 20dB. It is less significant in case of higher SNR-values, like 40dB.

3.2 Frequency-domain datasets

In this subsection, the analytical FRF of the single-degree of freedom system with real valued modal parameters from Table 1 is synthesized. The full frequency range is from 0 Hz to 12.5 Hz with a frequency resolution of 0.1 Hz. An analysis frequency band is typically selected for modal analysis. In order to allow the transfer of findings of this study to other cases of modal analysis, the band limits shall not be selected arbitrarily. Instead, the frequency band selected around the resonance peak of the FRF is a multiple of the half-power-bandwidth $B=2D_rf_r$ of the resonance peak. In this case, the analysis frequency band is centered around the resonance peak and ranges from $(f_r\text{-}2B) \leq f \leq (f_r+2B)$.

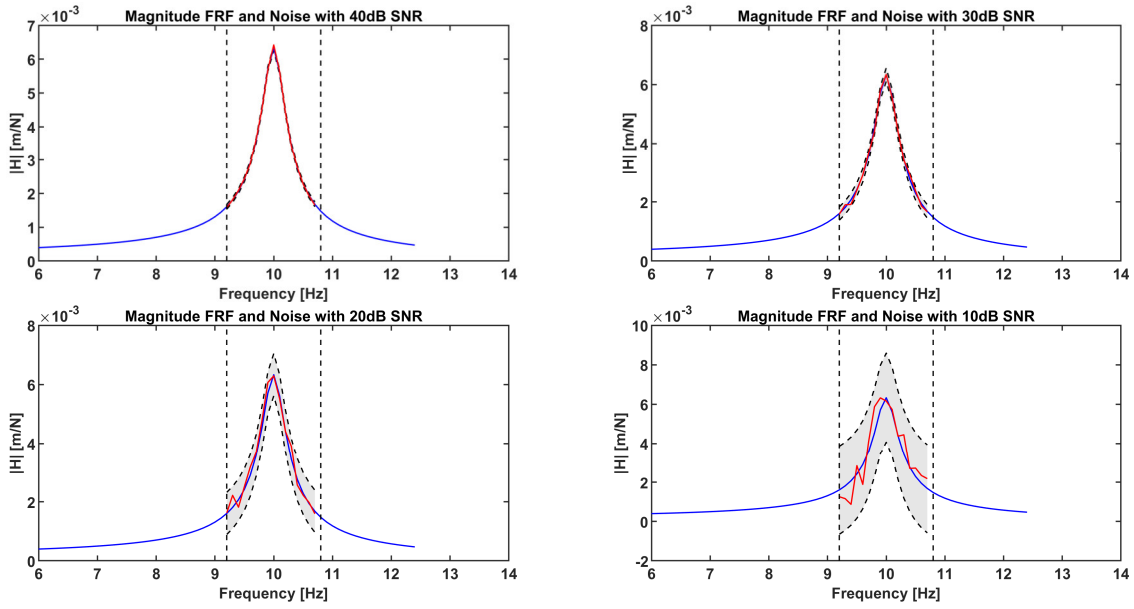


Figure 1: Magnitude of analytical FRF, noise contaminated FRF with different SNR in selected analysis frequency band with 95% confidence interval from 5000 realizations

The analysis frequency band comprises 16 spectral lines of the FRF. To the complex data of these 16 spectral lines zero mean Gaussian white noise is added independently to the real part and the imaginary part of the FRF. With the noise-free analytical FRF in the analysis band and the noise data, the SNR can be evaluated according to equation (6). Afterwards, the complex noise is scaled such that a target SNR value is reached. This is repeated 5000 times to provide 5000 realizations of the noise contaminated FRF, all having the same SRN. In addition, this process is repeated for different target levels of SNR. Figure 1 shows the examples of the noise contamination in case of 40 dB, 30 dB, 20 dB and 10 dB SNR. The blue curve is the analytical FRF of the single-degree of freedom system. The red curve is one realization of the noise contaminated FRF. The grey shaded area framed by the black dashed line is the 95 % confidence interval of the magnitude FRF according to ±1.96 σ of the 5000 realizations of noise contamination. Narrow confidence intervals can be observed e.g. for SNR=40 dB, while the confidence interval becomes wide e.g. for SNR=10 dB.

3.3 Time-domain datasets

When IRFs are used as input for time-domain modal analysis, quite often the selected frequency-domain response data in the analysis band is transformed back into the time-domain by means of inverse DFT. Since the analytical IRF can be synthesized with the given modal parameters, inverse DFT is not used, but instead, the analytical IRF is used directly. Discretization in time-domain and frequency-domain are strongly coupled and the parameters used in both domains are summarized in Table 2.

Table 2: Parameters for discretization of analytical response data in time- and frequency-domain

Eigen-frequency	Sampling Frequency	Sampling Interval	Block Length	Measurement Duration	Frequency Resolution
$f_r=\omega_r / (2\pi)$	$f_s=1 / \Delta t$	Δt	N	T	$\Delta f=1 / T$
10 Hz	25 Hz	0.04 s	250	10 s	0.1 Hz

In order to provide an equivalent amount of information for time-domain modal analysis as is used for frequency-domain modal analysis, the number of sampling points of the IRF is derived from the number of spectral lines in the analysis frequency band. 16 complex valued data points lie within the analysis frequency band as shown in Figure 1. Therefore, 32 real valued data points of the IRF are being used. This is illustrated on behalf of the analytical FRF and IRF in Figure 2, where the red colored part indicates the data used.

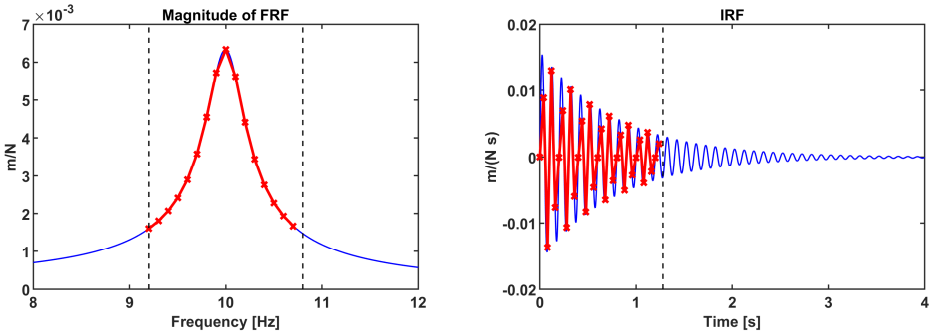


Figure 2: Left: Magnitude of analytical FRF (blue) and analysis frequency band (red), right: Analytical IRF (blue) and corresponding data points in analysis time interval (red)

For the generation of stochastic datasets in the time-domain, zero mean Gaussian white noise is added to the first 32 real valued data points of the analytical IRF. With the first 32 data points of the noise-free analytical IRF and the noise data, the SNR can be evaluated according to equation (5). Afterwards, the noise is scaled such that a target SNR value is reached. This is repeated 5000 times to provide 5000 realizations of the noise contaminated IRF. In addition, this is repeated for different target levels of SNR values. Figure 3 shows the examples of the noise contamination for 40 dB, 30 dB, 20 dB and 10 dB SNR. The blue curve is the analytical IRF of the single-degree of freedom system. The red curve is one realization of the noise contaminated IRF. The grey shaded area framed by the black dashed line is the 95 % confidence interval of the IRF according to $\pm 1.96\,\sigma$ of the 5000 realizations of noise contamination. Again, narrow confidence intervals can be observed e.g. for SNR=40 dB and a wide confidence interval for SNR=10 dB.

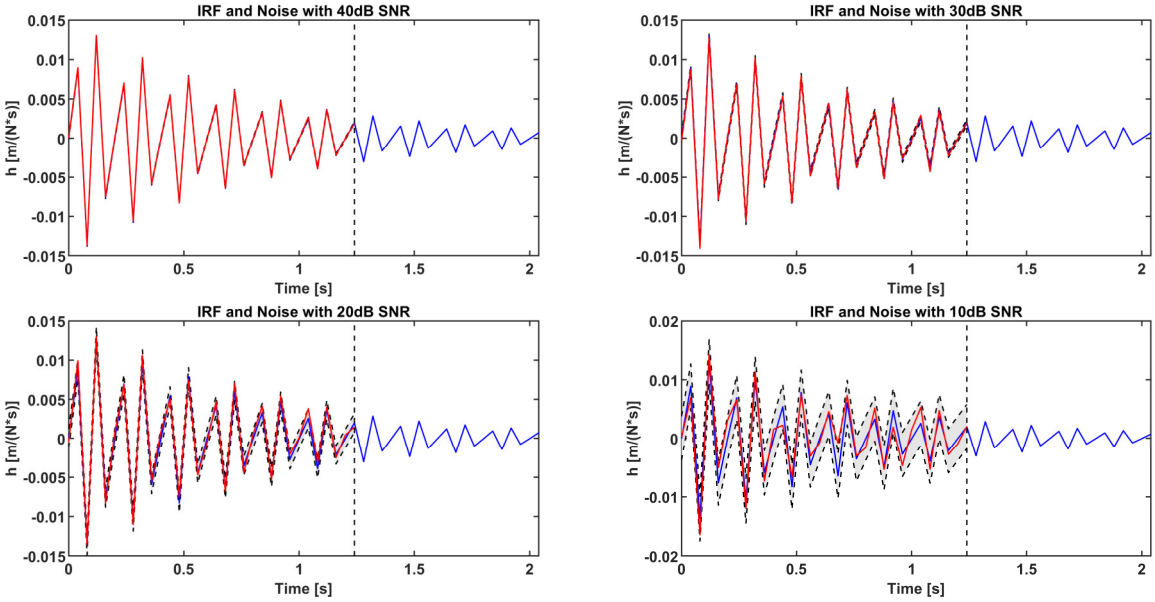


Figure 3: Analytical IRF, noise contaminated data with different SNR in selected analysis time interval with 95% confidence interval from 5000 realizations

4 Analysis of stochastic datasets

In this section, the results obtained from the stochastic datasets for time-domain and frequency-domain modal analysis will be presented. The identified mean values and the corresponding bias and coefficient of variation will be shown for different modal parameters, like undamped eigenfrequency ω_r, damping ratio D_r, residue $R_{kl,r}=(\phi_{k,r}\cdot\phi_{l,r})/m_r$ and modal mass m_r for the 5000 realizations of noise contaminated input data with different SNR values. The bias is the relative error of the mean value with respect to the analytical value. The coefficient of variation is the standard deviation divided by the mean value. In addition, the coefficient of correlation is presented for the eigenfrequency estimates and the damping ratio estimates.

4.1 Least-Squares Complex Frequency-Domain

The model order of the analytical system to be identified is known. It is set to $2n=2$ for modal analysis using LSCF. This means that 2 complex conjugate poles λ_r, $r=1,2$, are identified in the first step. The undamped eigenfrequency ω_r and the damping ratio D_r are extracted from the complex eigenvalue λ_r:

$$\omega_r = |\lambda_r| \quad , \quad D_r = -\frac{\lambda_r^{re}}{|\lambda_r|} \quad , \quad r = 1,2,\ldots,n \tag{7}$$

In the second step, the corresponding real valued mode shape vector $\{\phi_r\}$ and modal mass m_r are identified from curve-fitting the FRF using ω_r and D_r from the previous step.

The results for the identified eigenvalue for different SNR values are shown in Figure 4. A scatter cloud can be observed with the mean value from 5000 identifications indicated in green. The analytical eigenvalue is plotted in red. Two types of errors can be observed: i) bias is the systematic deviation of the mean value from 5000 identifications, ii) scatter is a stochastic dispersion of many identifications around the mean value. The scatter increases for both, real part eigenvalue and imaginary part eigenvalue, as the SNR decreases.

Figure 5 shows the corresponding scatter clouds when the results are presented as damping ratio D_r over undamped eigenfrequency f_r. It can be observed that the scatter of the damping ratio is much more significant than the scatter of the undamped eigenfrequency. This confirms the assertion that the eigenfrequency can

be identified more accurately than the damping ratio. The plots in Figure 5 also confirm the observations for the trend towards too low damping ratio in case of LSCF as the noise level increases. An analytical explanation for this effect was presented in [10].

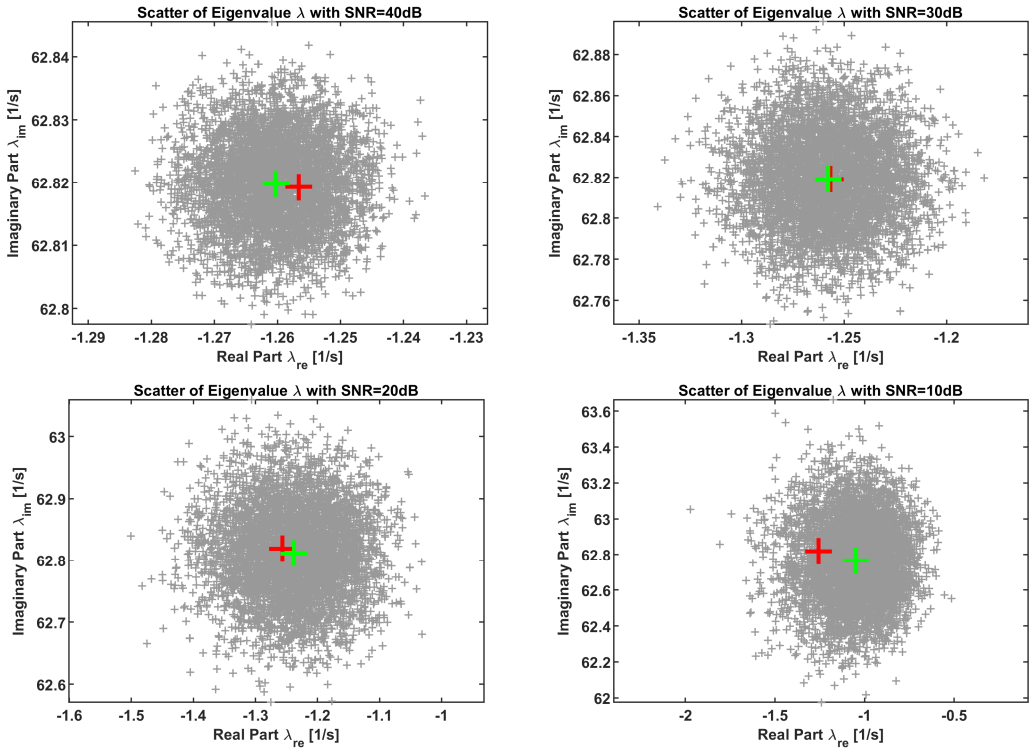


Figure 4: LSCF results for identified complex eigenvalue from 5000 analyses (grey) for different SNR values, mean value (green), analytical eigenvalue (red)

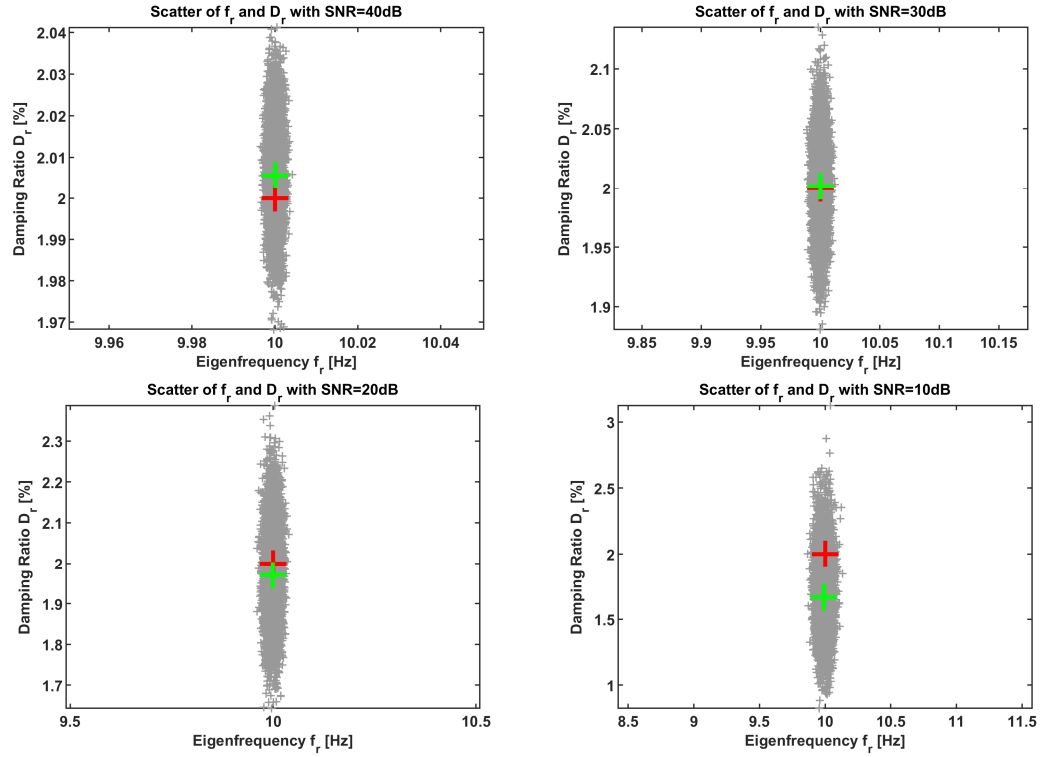


Figure 5: LSCF results for identified undamped eigenfrequency f_r and amping ratio D_r from 5000 analyses (grey) for different SNR values, mean value (green), analytical eigenvalue (red)

A summary of the mean values with the ±1.96 σ covariance ellipses for different SNR levels are presented in Figure 6. From the orientation of the covariance ellipses, one can conclude that there is a weak correlation of the respective stochastic quantities. Finally, the summary of all observations is presented in Table 3. In the right column, the coefficient of correlation is indicated among the eigenfrequency and the damping ratio.

Table 3: Summary of results accuracy of LSCF method for different SNR

		f_r	D_r	R_{kl}	m_r	Corr. f_r , D_r
10 dB	**Mean Value**	9.9909 Hz	1.6685 %	0.8864 kg^{-1}	1.1455 kgm^2	-2.4748 %
	Bias	-0.0906 %	-16.5736 %	-11.3619 %	14.5530 %	
	CoV	0.3581 %	17.0515 %	12.3057 %	12.4945 %	
20 dB	**Mean Value**	9.9987 Hz	1.9705 %	0.9902 kg^{-1}	1.0113 kgm^2	0.5380 %
	Bias	-0.0132 %	-1.4764 %	-0.9792 %	1.1319 %	
	CoV	0.1140 %	5.5569 %	3.7625 %	3.7628 %	
30 dB	**Mean Value**	10.000 Hz	2.0018 %	1.0004 kg^{-1}	0.9997 kgm^2	0.7845 %
	Bias	4.4e-05 %	0.0905 %	0.0406 %	-0.0262 %	
	CoV	0.0358 %	1.805 %	1.2004 %	1.2002 %	
40 dB	**Mean Value**	10.0001 Hz	2.0057 %	1.0016 kg^{-1}	0.9984 kgm^2	-1.2227 %
	Bias	0.0010 %	0.2836 %	0.1642 %	-0.1626 %	
	CoV	0.0112 %	0.5577 %	0.3718 %	0.3718 %	

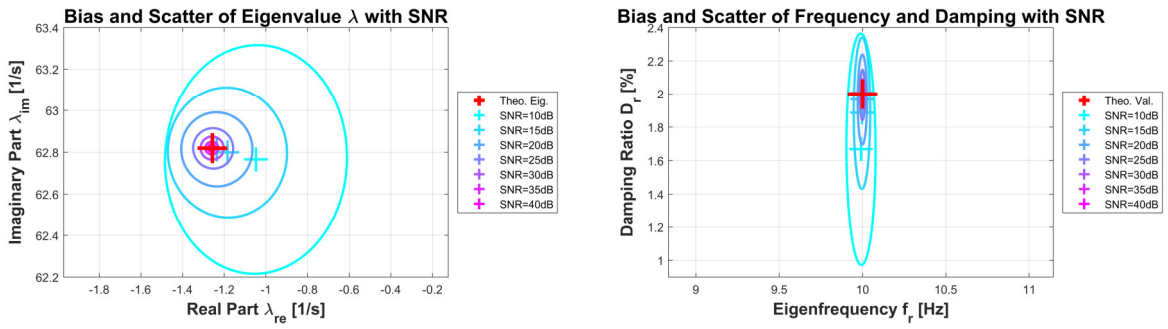


Figure 6: LSCF trends for mean value of identified complex eigenvalue, undamped eigenfrequency and damping ratio with corresponding covariance ellipses

4.2 Least-Squares Complex Exponential

The model order of the analytical system is known. Therefore, the model order for the modal analysis using LSCE is set to $2n=2$. This means that 2 complex conjugate poles λ_r, $r=1,2$ are identified in the first step. The undamped eigenfrequency ω_r and the damping ratio D_r are extracted from the complex eigenvalue λ_r according to equation (7). In the second step, the corresponding complex valued mode shape vector $\{\psi_r\}$ and complex modal a_r are identified by curve fitting the IRF. The real valued mode shape vector $\{\phi_r\}$ is obtained from its complex counterpart, assuming unity maximum component scaling for $\{\psi_r\}$:

$$\{\phi_r\} = \Re\left(\{\psi_r\}\right) = \left\{\psi_r^{re}\right\} \quad , \quad r = 1,2,\ldots,n \tag{8}$$

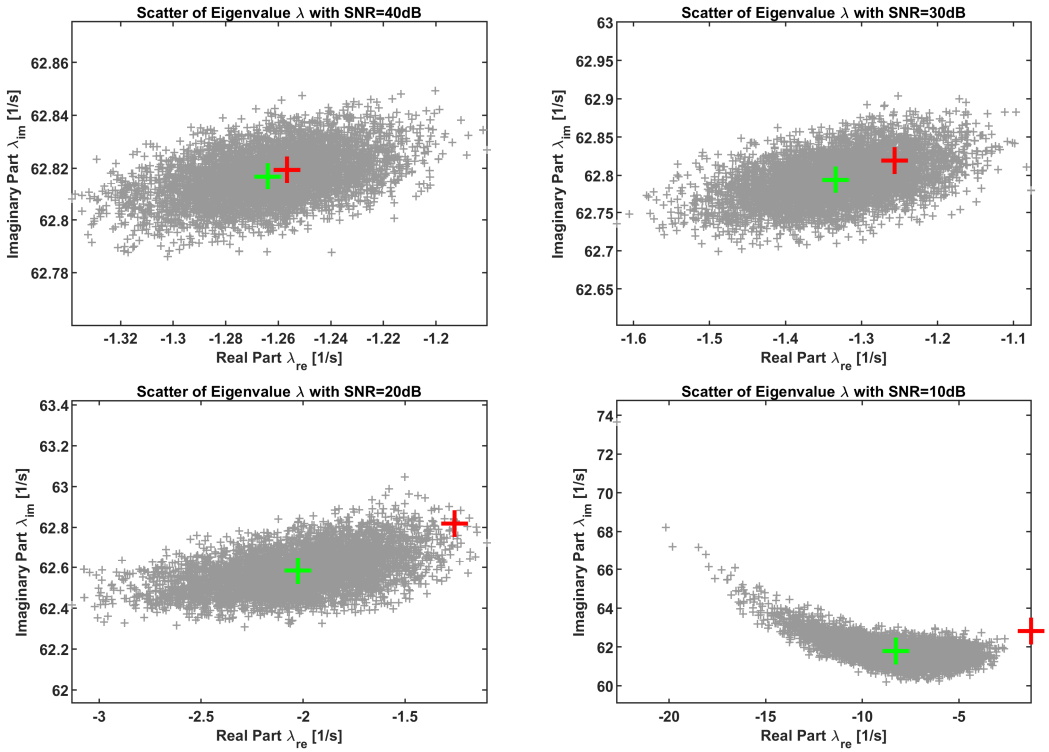


Figure 7: LSCE results for identified complex eigenvalue from 5000 analyses (grey) for different SNR values, mean value (green), analytical eigenvalue (red)

The real valued modal mass m_r is obtained from the complex modal a_r and the complex eigenvalue λ_r:

$$m_r = \frac{a_r^{im}}{2 \cdot \lambda_r^{im}} = \frac{a_r^{im}}{2 \cdot \omega_r \sqrt{1 - D_r^2}} \quad , \quad r = 1, 2, \ldots, n \tag{9}$$

The results for the identified eigenvalue for different SNR values are shown in Figure 7. A scatter cloud can be observed with the mean value from 5000 identifications indicated in green. The analytical eigenvalue is plotted in red. Two types of errors can be observed: i) bias is the systematic deviation of the mean value from 5000 identifications, ii) the scatter is the stochastic dispersion of many estimates around the mean value. The scatter increases for both, real and imaginary part, as the SNR decreases. Furthermore, it can be observed that the orientation of the scatter clouds is different compared to Figure 4. It seems that the identifications of real part and imaginary part eigenvalue are no longer uncorrelated. In addition, in case of poor SNR, the scatter cloud does not even have elliptical shape anymore. This indicates that the results are no longer independent stochastic variables with Gaussian normal distribution. Figure 8 shows the corresponding scatter clouds from LSCE when the results are presented as damping ratio D_r over undamped eigenfrequency f_r. Again, it can be observed, that the scatter of the damping ratio is much more significant than the scatter of the eigenfrequency.

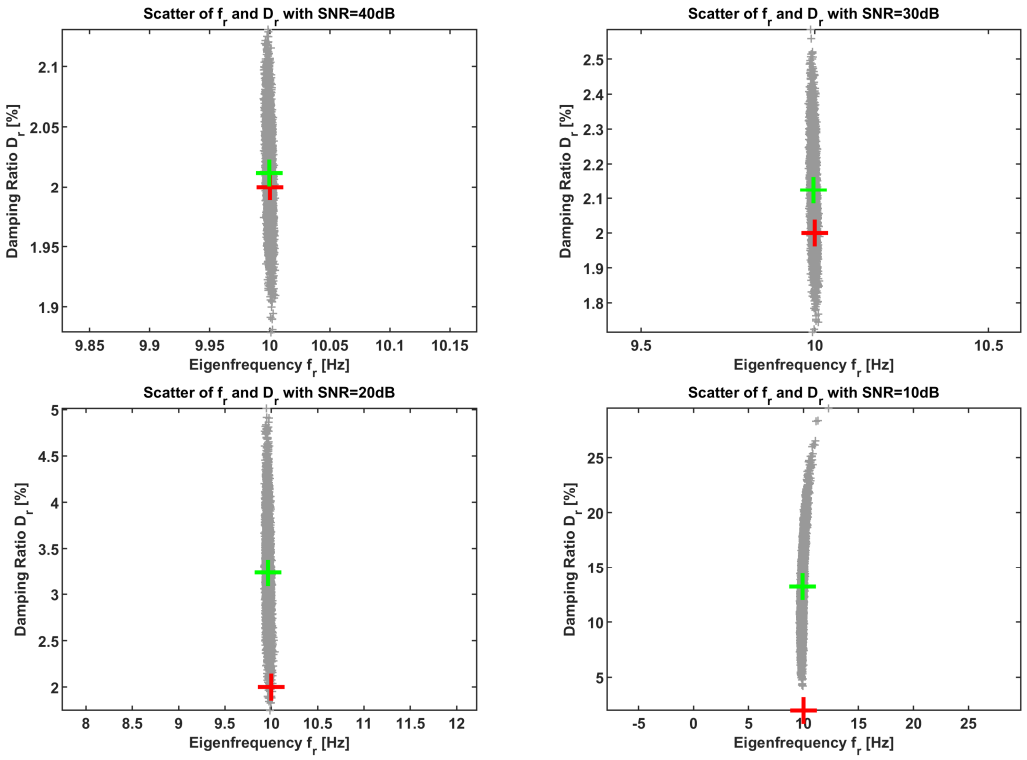


Figure 8: LSCE results for identified undamped eigenfrequency f_r and amping ratio D_r from 5000 analyses (grey) for different SNR values, mean value (green), analytical eigenvalue (red)

A summary of the mean values with the ±1.96 σ covariance ellipses for different SNR levels is presented in Figure 9. There is a change in the orientation of the covariance ellipse from SNR=10 dB to SNR=15 dB. This can be attributed to the non-elliptical shape of the scatter cloud in case of SNR=10 dB. Finally, the summary of all observations is presented in Table 4. The right column indicates the strong correlation among the identified eigenfrequency and damping ratio. The correlation coefficient changes sign with the highest noise level SNR=10dB. This is confirmed by the different orientation of the covariance ellipse for this SNR-level as compared to the other levels. It should be noted, however, that a fit of the corresponding scatter cloud in Figure 7, or respectively Figure 8, with an ellipse is questionable in this case.

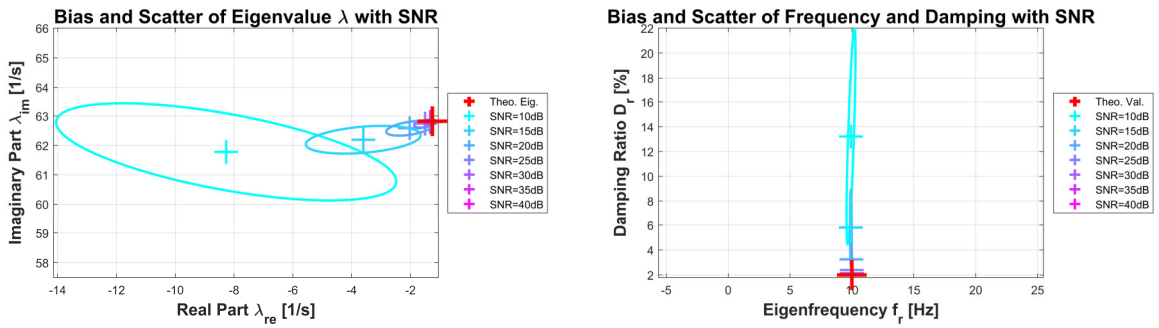


Figure 9: LSCE trends for mean value of identified complex eigenvalue, undamped eigenfrequency and damping ratio with corresponding covariance ellipses

Table 4: Summary of results accuracy of LSCE method for different SNR

		f_r	D_r	R_{kl}	m_r	Corr. f_r , D_r
10 dB	**Mean Value**	9.9268 Hz	13.2149 %	2.0704 kg^{-1}	0.4948 kgm²	76.3955 %
	Bias	-0.7322 %	560.7462 %	107.0409 %	-50.5188 %	
	CoV	1.4966 %	27.1147 %	18.2597 %	14.6681 %	
20 dB	**Mean Value**	9.9658 Hz	3.2347 %	1.2286 kg^{-1}	0.8180 kgm²	-38.8792 %
	Bias	-0.3416 %	61.7346 %	22.8625 %	-18.2026 %	
	CoV	0.1549 %	16.0831 %	6.9894 %	7.1275 %	
30 dB	**Mean Value**	9.9962 Hz	2.1242 %	1.0264 kg^{-1}	0.9750 kgm²	-42.1648 %
	Bias	-0.0376 %	6.2100 %	2.6362 %	-2.4984 %	
	CoV	0.0481 %	5.9899 %	2.6776 %	2.6841 %	
40 dB	**Mean Value**	9.9996 Hz	2.0118 %	1.0025 kg^{-1}	0.9976 kgm²	-40.4867 %
	Bias	-0.0039 %	0.5884 %	0.2524 %	-0.2444 %	
	CoV	0.0148 %	1.9305 %	0.8590 %	0.8591 %	

4.3 Eigensystem Realization Algorithm

The model order of the analytical system is known. Therefore, the parameters for the size of the two Hankel matrices $[Y_0]$ and $[Y_1]$ used by ERA (see e.g. chapter 5.5.4 in [3]) are set to $\alpha=4$ and $\beta=11$:

$$[Y_0] = \begin{bmatrix} \{y_1\} & \{y_2\} & \cdots & \{y_\beta\} \\ \{y_2\} & \{y_3\} & \vdots & \{y_{\beta+1}\} \\ \vdots & \vdots & \ddots & \vdots \\ \{y_\alpha\} & \{y_{\alpha+1}\} & \cdots & \{y_{\alpha+\beta-1}\} \end{bmatrix}, [Y_1] = \begin{bmatrix} \{y_2\} & \{y_3\} & \cdots & \{y_{\beta+1}\} \\ \{y_3\} & \{y_4\} & \vdots & \{y_{\beta+2}\} \\ \vdots & \vdots & \ddots & \vdots \\ \{y_{\alpha+1}\} & \{y_{\alpha+2}\} & \cdots & \{y_{\alpha+\beta}\} \end{bmatrix} \quad (10)$$

The parameter α is required to obtain 2 conjugate complex eigenvalues. The parameter β has been adjusted accordingly in order to use as much as possible from the 32 response data points available for this study.

ERA identifies complex modal parameters. The undamped eigenfrequency ω_r and the damping ratio D_r are extracted from the complex eigenvalue λ_r according to equation (7). The real valued mode shape vector $\{\phi_r\}$ is obtained from its complex counterpart by using equation (8). The real valued modal mass m_r is obtained from the complex modal a_r and the complex eigenvalue λ_r using equation (9).

The results for the identified eigenvalue for different SNR values are shown in Figure 10. Only three diagrams are shown there, because the ERA method could not provide results for SNR=15 dB and for SNR=10 dB. A scatter cloud can be observed with the mean value from 5000 identifications indicated in green. The analytical eigenvalue is plotted in red. The bias is almost not visible. The scatter increases for both, real and imaginary part, as the SNR decreases. In all cases, the shape of the scatter cloud is elliptic and the orientation of the main diagonals of the covariance ellipse suggests that real and imaginary part eigenvalue are almost uncorrelated. Figure 11 shows the corresponding scatter clouds when the results are presented as damping ratio D_r over undamped eigenfrequency f_r. Again, it can be observed, that the scatter of the damping ratio is much more significant than the scatter of the eigenfrequency.

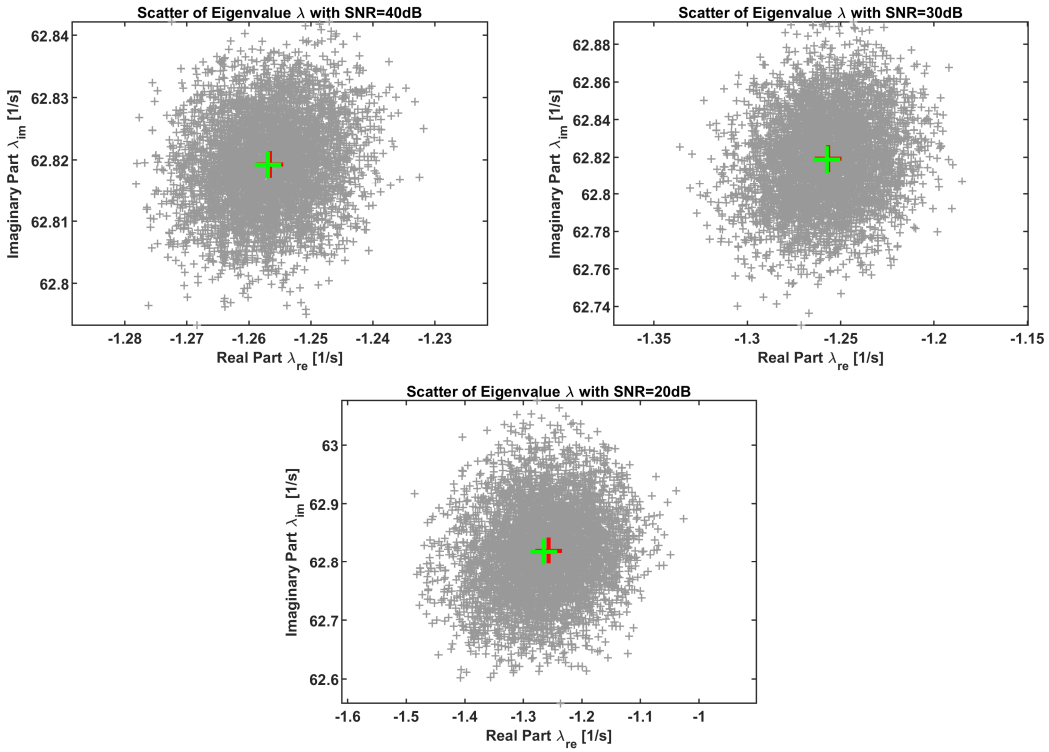


Figure 10: ERA results for identified complex eigenvalue from 5000 analyses (grey) for different SNR values, mean value (green), analytical eigenvalue (red)

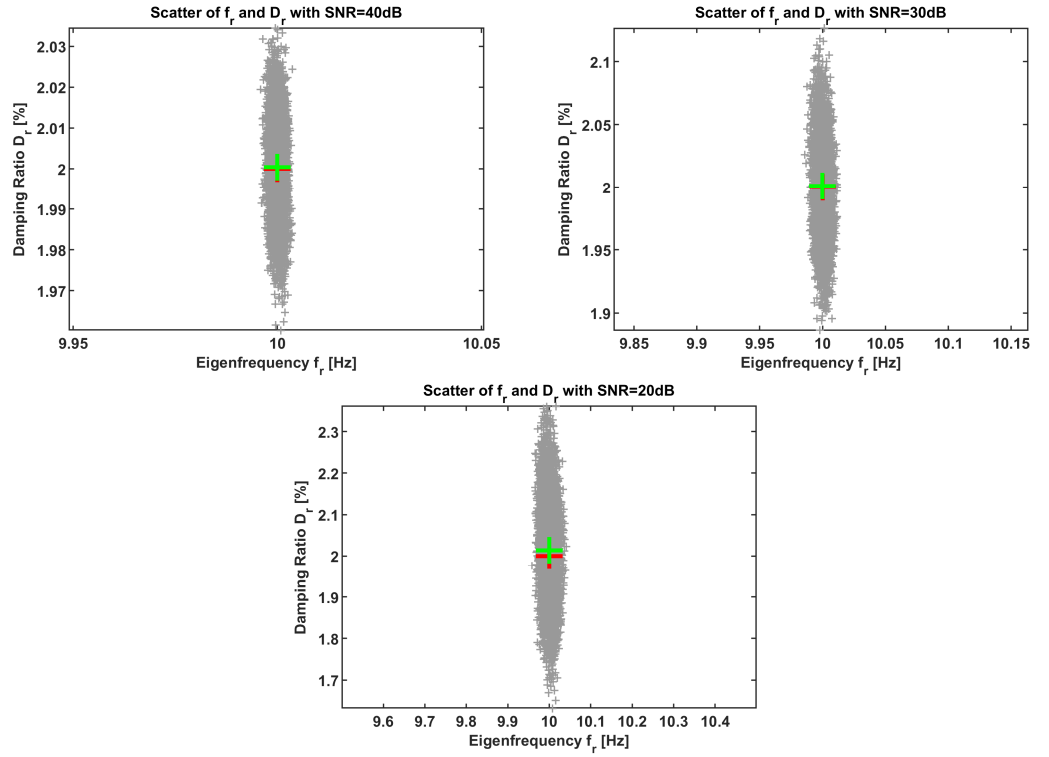


Figure 11: ERA results for identified undamped eigenfrequency f_r and amping ratio D_r from 5000 analyses (grey) for different SNR values, mean value (green), analytical eigenvalue (red)

A summary of the mean values with the ±1.96 σ covariance ellipses for different SNR levels is presented in Figure 9. Finally, the summary of all observations is presented in Table 5.

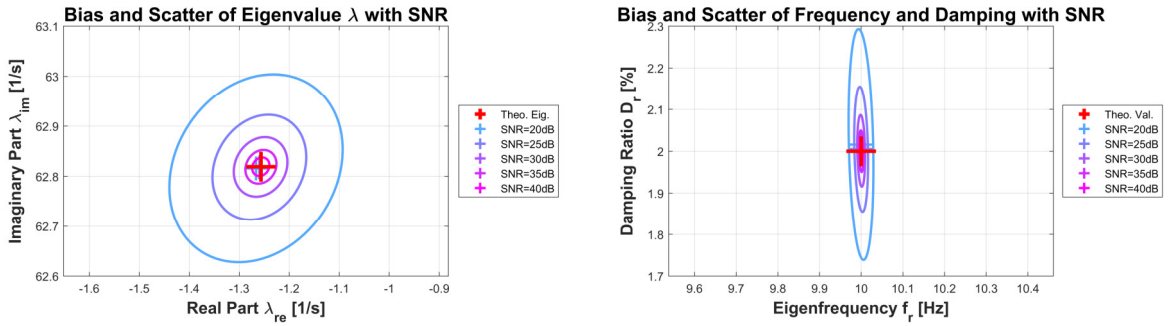


Figure 12: ERA trends for mean value of identified complex eigenvalue, undamped eigenfrequency and damping ratio with corresponding covariance ellipses

Table 5: Summary of results accuracy of ERA method for different SNR

		f_r	D_r	R_{kl}	m_r	Corr. f_r , D_r
10 dB	**Mean Value**	N/A	N/A	N/A	N/A	N/A
	Bias	N/A	N/A	N/A	N/A	
	CoV	N/A	N/A	N/A	N/A	
20 dB	**Mean Value**	9.9998 Hz	2.0136 %	1.0016 kg^{-1}	0.9991 kgm^2	-15.2586 %
	Bias	-0.0020 %	0.6790 %	0.1614 %	-0.0950 %	
	CoV	0.1213 %	5.6041 %	2.5716 %	2.5758 %	
30 dB	**Mean Value**	9.9999 Hz	2.0011 %	1.0016 kg^{-1}	0.9985 kgm^2	-16.3073 %
	Bias	-0.0007 %	0.0569 %	0.1594 %	-0.1526 %	
	CoV	0.0385 %	1.7489 %	0.8103 %	0.8103 %	
40 dB	**Mean Value**	10.0000 Hz	2.0004 %	1.0016 kg^{-1}	0.9984 kgm^2	-16.7845 %
	Bias	-0.0001 %	0.0218 %	0.1595 %	-0.1586 %	
	CoV	0.0119 %	0.5620 %	0.2565 %	0.2565 %	

5 Discussion of results and outlook

The LSCE method exhibits a significant bias, particularly in the estimation of the damping ratio. The results accuracy can be improved considerably in terms of bias and in terms of scatter by increasing the model order, see e.g. Figure 13. However, for the sake of comparability, the model order was the same for all three methods in chapter 4. In addition, higher model orders result in the identification of additional (spurious) eigenvalues, requiring additional effort to distinguish and select the desired eigenvalue from the set of identified candidates.

Both, the LSCF and ERA method provide very accurate results under favorable conditions. ERA has less bias in the damping estimates compared to LSCF while the scatter of damping ratios is about the same for the two methods. Nevertheless, the ERA method failed when the signal-to-noise ratio (SNR) is too low. In case of the LSCF method, an additional bias in the estimated eigenfrequency can occur when the resonance peak is not properly centered within the selected analysis frequency band. This effect has been discussed in [10] and an analytical has been given.

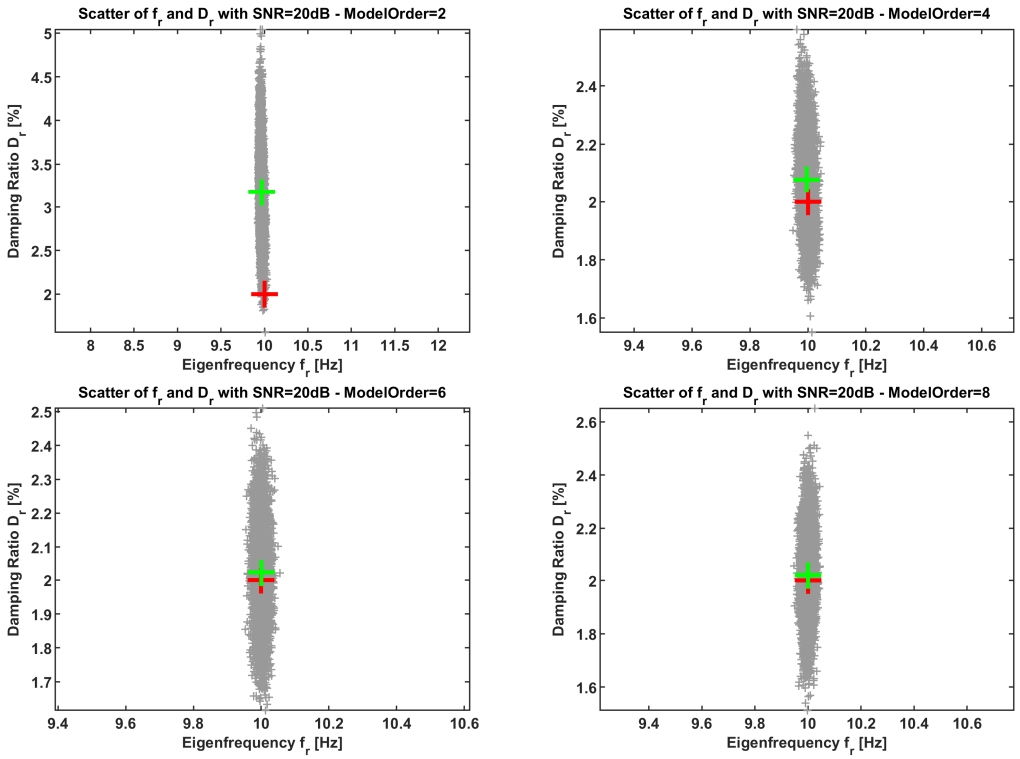


Figure 13: LSCE results for eigenfrequency f_r and damping ratio D_r from 5000 analyses (grey) for 20dB SNR and increasing model order $2n=2, 4, 6, 8$

It should be pointed out that in case of the modal methods (i.e. LSCF and LSCE) there is correlation between the biases in damping ratio and modal mass. When damping is estimated too low, the modal mass is too high and vice versa. This effect is due to the sequential steps in the analysis process. In both methods, the eigenvalue is identified in the first step. In the second step, the residue is identified from curve fitting. Here, the previously identified eigenvalue is used. Thus, a possible error in real part eigenvalue will lead to an error in the identification of the residue and consequently to an error in the modal mass. This is not observed in case of direct methods (i.e. ERA).

Next, the meaning of the results of this study shall be discussed for practical applications in experimental modal analysis. With the findings of this study, the results accuracy of different modal analysis methods can be assessed, provided that the SNR of the input data can be estimated e.g. based on noise floor measurements in the absence of excitation. The information provided by this study shall enable the operator of modal analysis to select the appropriate analysis method based on the input data quality available and on the requirements on results accuracy of experimental modal analysis.

It is planned to verify the findings of this study on measured modal analysis test cases from multi-degree of freedom systems. When some resonance peaks appear isolated in the FRFs of multi-degree of freedom systems, for example, the SNR in the $\pm 2B$-vicinity of the respective resonance peak can be estimated. It is envisaged that bias and scatter of the results are compared to the results of the study presented here.

Of course, the methodology presented here can be repeated also for further modal analysis methods, e.g. FDPI which is a direct method in the frequency-domain, and also for different amounts of data points used for modal analysis. The system used for the investigations is documented here and researchers are encouraged to contribute with further research and findings.

Finally, the results of this study should enable engineers in charge of experimental modal analysis to assess the expected accuracy of the different types of modal parameters they have obtained based on the estimated SNR of noisy datasets.

References

[1] E. Reynders, K. Maes, G. Lombaert, G. De Roeck, “Uncertainty quantification in operational modal analysis with stochastic subspace identification: Validation and applications,” *MSSP*, vol. 66-67, pp. 13-30, 2016, http://dx.doi.org/10.1016/j.ymssp.2015.04.018.

[2] T. De Troyer, P. Guillaume, R. Pintelon, S. Vanlanduit, “Fast calculation of confidence intervals on parameter estimates of least-squares frequency-domain estimators,” *MSSP*, vol. 23, pp. 261-273, 2009, http://dx.doi.org/10.1016/j.ymssp.2008.04.009.

[3] M. Böswald, *Modalanalyse in der Strukturdynamik - Theoretische Grundlagen, experimentelle Methoden, Anwendungen in experimenteller und operationeller Modalanalyse*. Springer Vieweg, Wiesbaden, 2026.

[4] D.L. Brown, R.J. Allemang, and R. Zimmerman, "Parameter Estimation Techniques for Modal Analysis," in *Automotive Engineering Congress and Exposition*, SAE Technical Paper 790221, 1979, https://doi.org/10.4271/79022.

[5] J.N. Juang, and R.S. Pappa, "An Eigensystem Realization Algorithm for Modal Parameter Identification and Model Reduction," *J. Guid. Control Dyn*., vol. 8, no. 5, pp. 620-627, 1985.

[6] P. Guillaume, P. Verboven, S. Vanlanduit, H. van der Auweraer, and B. Peeters, "A polyreference implementation of the least-squares complex frequency-domain estimator," in *21st International Modal Analysis Conference*, IMAC XXI, Kissimmee, Florida, 3-6 February, 2003.

[7] A. Brandt, *Noise and Vibration analysis: signal analysis and experimental procedures*. 2nd edition, Wiley, Chichester, UK, 2023

[8] J.N. Juang, *Applied system identification*. Prentice Hall, Upper Saddle River, NJ, 1994

[9] R. Pintelon, J. Schoukens, *System Identification - A Frequency-Domain Approach*. IEEE Press, Piscataway, New Jersey, 2001.

[10] M. Böswald, "Analysis of the bias in modal parameters obtained with frequency-domain rational fraction polynomial estimators," in *Proceedings of the International Conference on Noise and Vibration Engineering, ISMA 2016*, Leuven, Belgium, 2016, pp. 2907-2921.